Available online at www.sciencedirect.com

SciVerse ScienceDirect

Ceramics International 39 (2013) 1533–1538

CERAMICS INTERNATIONAL

www.elsevier.com/locate/ceramint

Synthesis and characterization of rhombohedral- and tetragonal-lanthanum oxyfluoride powders

Dong Chan Woo[a], Min-Ho Lee[b], Woo-Sik Jung[b,*]

[a]School of Materials Science and Engineering, College of Engineering, Yeungnam University, 214-1 Dae-dong, Gyongsan 712-749, Republic of Korea
[b]School of Chemical Engineering, College of Engineering, Yeungnam University, 214-1 Dae-dong, Gyongsan 712-749, Republic of Korea

Received 5 June 2012; received in revised form 30 July 2012; accepted 30 July 2012
Available online 7 August 2012

Abstract

Rhombohedral- and tetragonal-lanthanum oxyfluoride (LaOF) powders were prepared by thermal decomposition of lanthanum(III) carbonate fluoride ($LaFCO_3$) powders that had been obtained from boiling an aqueous solution containing lanthanum(III) salt, fluoride ion (F^-), and urea. The conversion process of $LaFCO_3$ to LaOF was monitored by thermogravimetry, powder X-ray diffraction, and ^{19}F magic-angle spinning nuclear magnetic resonance spectroscopy. The crystal structure (rhombohedral, tetragonal) of LaOF depended on the mole ratio of F^- to La^{3+} ions in the preparation of $LaFCO_3$, and tetragonal-LaOF was completely transformed into rhombohedral-LaOF at 1000 °C. The difference in crystal structures was reflected in the intensity of the $^5D_0 \rightarrow {}^7F_0$ transition peak in the luminescence spectra of Eu^{3+}-doped LaOF powders.

Keywords: Synthesis; LaOF; $LaFCO_3$; Eu^{3+}-doping

1. Introduction

Lanthanum oxyfluoride (LaOF) has attracted extensive interest as a host material of phosphors [1–9], a catalyst for oxidative coupling of methane [10], and a solid electrolyte [11,12]. LaOF powders and thin films have been prepared by various methods, including solid-state reaction between lanthanum oxide (La_2O_3) and lanthanum(III) fluoride (LaF_3) [10–15] or ammonium fluoride (NH_4F) [8,16], ball milling and calcination of a mixture of La_2O_3 and polytetrafluoroethylene [17,18], annealing of LaF_3 in air [1,2,6], sol–gel method [3,4,9], decomposition of lanthanum(III) trifluoroacetate in boiling oleylamine [5], and thermal decomposition of lanthanum(III) carbonate fluoride ($LaFCO_3$) in air [7]. Two room-temperature crystal structures of LaOF, rhombohedral and tetragonal [19], can be controlled by the annealing temperature [3,6,7] and/or the mole ratio of F^- to La^{3+} ions in the precursors [8,12,16]. To date, the two crystal structures of LaOF powders have usually been identified by powder X-ray diffraction (XRD), but their discrimination by XRD is often ambiguous because of the similarity in their XRD patterns. Furthermore, it is impossible to identify the crystal structure of low-crystalline and/or nanosized LaOF powders by XRD due to their broad diffraction peaks [5,9,13]. Hölsä et al. showed that the change in the crystal structure of LaOF was accompanied by significant modifications in the Raman and infrared spectra [16].

In this study, LaOF powders were obtained by thermal decomposition of $LaFCO_3$ powder, which was previously prepared from boiling an aqueous solution containing lanthanum(III) salt, F^- ion, and urea while varying the mole ratio of F^- to La^{3+} ions. The resulting powders were characterized by powder XRD and ^{19}F magic-angle spinning nuclear magnetic resonance (MAS NMR) spectroscopy. To the best of our knowledge, this is the first report on characterization of LaOF powders by ^{19}F MAS NMR spectroscopy. Recently, Janka and Schleid prepared LaOF by thermal decomposition of $LaFCO_3$ powders, which had been obtained from a mixture of lanthanum(III) salt, F^- ion, and $NaHCO_3$ (in mole ratio of 1:1.3:1.3) in aqueous solution [7]. The luminescence spectrum of the dopant ion, such as Eu^{3+}, can be used to probe its local environment in the host crystal environment. The luminescence spectra

*Corresponding author. Tel.: +82 53 810 2528; fax: +82 53 810 4631.
E-mail address: wsjung@yu.ac.kr (W.-S. Jung).

0272-8842/$ - see front matter © 2012 Elsevier Ltd and Techna Group S.r.l. All rights reserved.
http://dx.doi.org/10.1016/j.ceramint.2012.07.103

of Eu^{3+}-doped LaOF ($LaOF:Eu^{3+}$) powders were also measured to investigate the difference of the crystal structure of LaOF.

2. Experimental procedure

2.1. Synthesis of $LaFCO_3$ (A) and (B)

All starting materials, $La(NO_3)_3 \cdot 6H_2O$ (99.9%), $Eu(NO_3)_3 \cdot 5H_2O$ (99.9%), NH_4F (>99.99%), and urea (99.0%), were purchased from Sigma-Aldrich Co. A solution of NH_4F (0.741 g, 2.00×10^{-2} mol) in 50 mL H_2O was added to a solution of $La(NO_3)_3 \cdot 6H_2O$ (8.660 g, 2.00×10^{-2} mol) in 20 mL H_2O, followed by the addition of urea (2.402 g, 4.00×10^{-2} mol). The mixed solution was boiled for 15 h. The precipitate was separated by centrifugation, washed with distilled water, and then dried in an oven. The product is referred to as $LaFCO_3$ (A). When the amount (0.962 g, 2.60×10^{-2} mol) of NH_4F (0.962 g, 2.60×10^{-2} mol) was used in the aforementioned procedure, the product is referred to as $LaFCO_3$ (B).

2.2. Synthesis of rhombohedral- and tetragonal-LaOF powders

LaOF powders were obtained by thermal decomposition of $LaFCO_3$ powders for 5 h in the temperature range between 500 and 1000 °C. The samples obtained by thermal decomposition of $LaFCO_3$ (A) and $LaFCO_3$ (B) powders at T °C are referred to as A-T and B-T, respectively.

2.3. Synthesis of $LaOF:Eu^{3+}$ powders

$LaOF:Eu^{3+}$ powders were obtained by thermal decomposition of $LaFCO_3:Eu^{3+}$ powders, which were prepared in the same way as $LaFCO_3$ powders except that $Eu(NO_3)_3 \cdot 5H_2O$ (4 mol%) was added to the solution of $La(NO_3)_3 \cdot 6H_2O$.

2.4. Product characterization

The thermogravimetric (TG) and differential thermal analysis (DTA) curves of $LaFCO_3$ were recorded on an SDT Q600 apparatus (TA Instruments) at a heating rate of 10 °C/min. The product powders obtained by thermal decomposition of $LaFCO_3$ powders were characterized by powder XRD with a PANalytical X'Pert PRO MPD X-ray diffractometer with Cu-Kα radiation operating at 40 kV and 30 mA and by high-resolution ^{19}F MAS NMR spectroscopy. The NMR spectra were measured at ambient temperature with a radio frequency of 564.5 MHz on a Unity INOVA 600 spectrometer. The samples were spun at 23 or 30 kHz. The chemical shifts (δ) were referenced to $CFCl_3$ at 0 ppm. The morphology of the product powders was investigated by scanning electron microscopy (SEM, Hitachi S-4200). The luminescence spectra of $LaFCO_3:Eu^{3+}$ and $LaOF:Eu^{3+}$ powders were measured at ambient temperature on a JASCO FP-6500 spectrofluorometer with a xenon lamp.

3. Results and discussion

3.1. Synthesis and characterization of LaOF

The TG curves of $LaFCO_3$ (A) and (B) indicated that the weight sluggishly decreased with increasing temperature up to *ca.* 300 °C and then abruptly decreased at *ca.* 400 °C (Fig. 1). The first sluggish step was attributed to the loss of occlusion water [7], and the second abrupt step to the reaction $LaFCO_3 \rightarrow LaOF + CO_2$, resulting in a theoretical weight loss of 20.2 wt%. The total weight losses for $LaFCO_3$ (A) and (B) were determined to be 21.8 and 18.7 wt%, respectively. The lower weight loss for $LaFCO_3$ (B) was due to the involvement of a small amount of LaF_3 (see below), which was transformed into LaOF with a theoretical weight loss of 11.2 wt%. The weight remained almost constant above 500 °C for both samples. The mole ratio of F^- to La^{3+} ions in the preparation of $LaFCO_3$ (B) was the same as that of $LaFCO_3$ in the Janka and Schleid's method [7]. The total weight loss for the former $LaFCO_3$ was similar to that for the latter $LaFCO_3$, whereas for $LaFCO_3$ (B) the step with a small weight loss of about 1% was not observed between 500 and 550 °C, as shown in Fig. 1(B). The DTA curves in Fig. 1 indicated that the endothermic peak for $LaFCO_3$ (A) appeared at the higher temperature than that for $LaFCO_3$ (B).

Fig. 2 shows the XRD patterns of samples obtained by thermal decomposition of $LaFCO_3$ (A) and (B) powders for 5 h in air at various temperatures. The XRD patterns of $LaFCO_3$ (A) and (B) powders corresponded to $LaFCO_3$ (ICDD-PDF #98-000-9727) and a mixture of $LaFCO_3$ and LaF_3 (ICDD-PDF #98-001-7194), respectively. The XRD pattern corresponding to LaF_3 was not observed for the $LaFCO_3$ powder obtained by Janka and Schleid [7]. The XRD patterns of A-500 and B-500 were very similar except for the very weak diffraction peaks observed at $2\theta = 40.3°$ and 37.8° for A-500 and B-500, respectively. The XRD

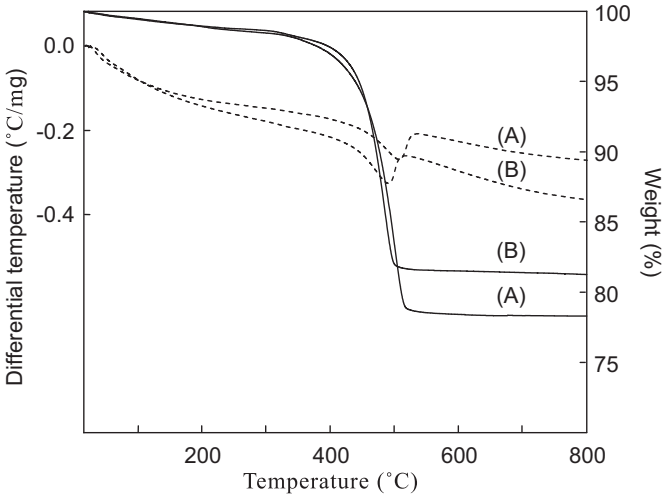

Fig. 1. TG (solid line) and DTA (dotted line) curves of $LaFCO_3$ powders obtained from (A) 1:1 and (B) 1.3:1 (in mole ratio) mixtures of F^- to La^{3+} ions.

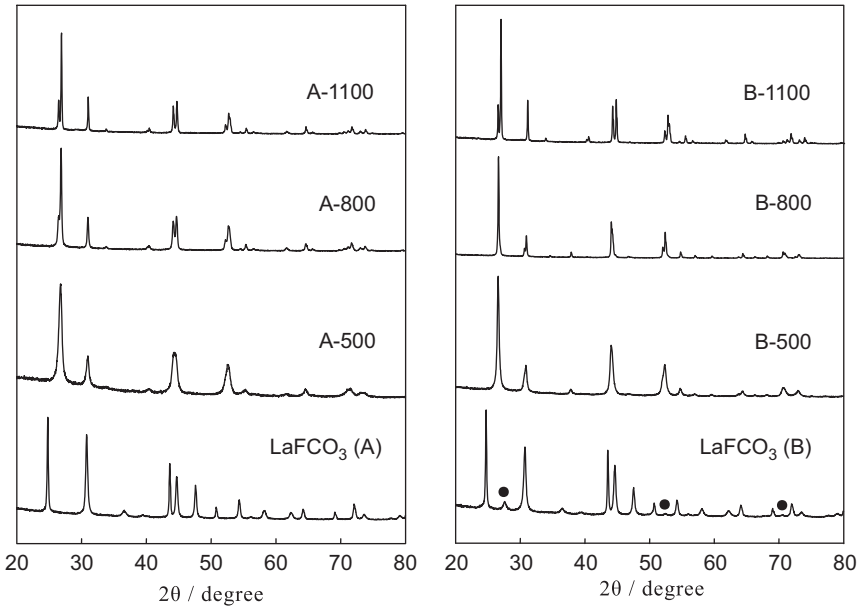

Fig. 2. XRD patterns of samples obtained by thermal decomposition of $LaFCO_3$ (A) and (B) powders for 5 h in air at various temperatures. (●) LaF_3.

patterns of A-800 and B-800, in which all diffraction peaks became narrower and more distinct than those of A-500 and B-500, were assigned to rhombohedral- (ICDD-PDF #01-075-1174) and tetragonal-LaOF (ICDD-PDF #01-089-5168), respectively. It is evident from these results that the crystal structure of LaOF depends on the mole ratio of F^- to La^{3+} ions in the preparation of $LaFCO_3$. Hölsä prepared rhombohedral- and tetragonal-LaOF powders by the solid state reaction between La_2O_3 and NH_4F, at mole ratios of 1:2 and $1:>2$, respectively, at 1050 °C in static ambient atmosphere [8]. The XRD pattern of B-1000 was the same as that of A-1000, indicating that tetragonal-LaOF was completely transformed to rhombohedral-LaOF at 1000 °C, a transformation temperature that was different from that for other reaction systems [3,6,7].

The thermal decomposition products of $LaFCO_3$ were also characterized by ^{19}F MAS NMR spectroscopy (Fig. 3). The ^{19}F MAS NMR spectrum of $LaFCO_3$ (A) exhibited one broad peak at 8 ppm. There are two different F^- sites in the bastnaesite-type $LaFCO_3$ [7]. The geometric structure around both F^- ions, which are threefold coordinated by La^{3+}, shows a subtle difference, resulting in the irresolution of NMR peaks corresponding to two different F^- ions. The ^{19}F MAS NMR spectrum of $LaFCO_3$ (B) was similar to that of $LaFCO_3$ (A) except that an additional peak was observed at δ −31 ppm. The additional peak was assigned to the F1 site, which is the most abundant site of three different F^- sites in the tysonite-structured LaF_3 [20]. The other two ^{19}F peaks of LaF_3 were observed as a shoulder on the high-frequency side of the ^{19}F peak of $LaFCO_3$.

The intense peak at δ −29 ppm in the NMR spectra of A-500, A-800, and A-1000 was assigned to four F^- ions coordinated to La^{3+} ion in rhombohedral-LaOF. The appearance of the weak peak at δ −38 ppm in the NMR spectrum of A-500 could not be deduced from the similarity in the XRD patterns of A-500 and A-800 (or A-1000). This weak peak, the chemical shift of which was similar to that of the normal F^- sites in tetragonal-LaOF, may be assigned to F^- sites in the distorted rhombohedral-LaOF structure. The crystal structure of LaOF can be considered as derived from that of the CaF_2 (fluorite) system by the resemblance in their XRD patterns, a resemblance that is most striking for the tetragonal-LaOF [8,19]. Therefore, the ^{19}F MAS NMR spectrum of tetragonal-LaOF was expected to resemble that of CaF_2. Wang and Grey observed four distinct peaks in the ^{19}F MAS NMR spectra of defect CaF_2 with F^- ion excess and assigned the peaks to three different types of sites including the interstitial sites [21]. The NMR spectra of B-500 and B-800 were similar in that three peaks were observed at δ −21, −29, and −39 ppm. As shown in Fig. 4, the deconvolution analysis using Gaussian peak components gave relative populations of three peaks: 0.04:0.22:0.74 for B-500 and 0.02:0.08:0.90 for B-800. The decreased intensities of the two peaks at the higher frequency with increasing temperature indicated that the peaks were due to excess F^- ions that occupy interstitial sites in nonstoichiometric tetragonal-LaOF structure [22], as for F^- ion-excess CaF_2. Interestingly, the ^{19}F MAS NMR spectra of tetragonal-LaOF and CaF_2 showed two common characteristics: the peaks corresponding to excess F^- sites were high-frequency shifted relative to the peak corresponding to the normal F^- sites and the difference in chemical shifts between adjacent peaks was in the range of 8–10 ppm. The spectrum of B-1000 was the same as that of A-1000, which was in agreement with the results of their XRD patterns.

The morphology of A-800 and B-800 was observed by SEM. As shown in Fig. 5, the particles of A-800 were homogeneously nanosized, despite being coalesced, with

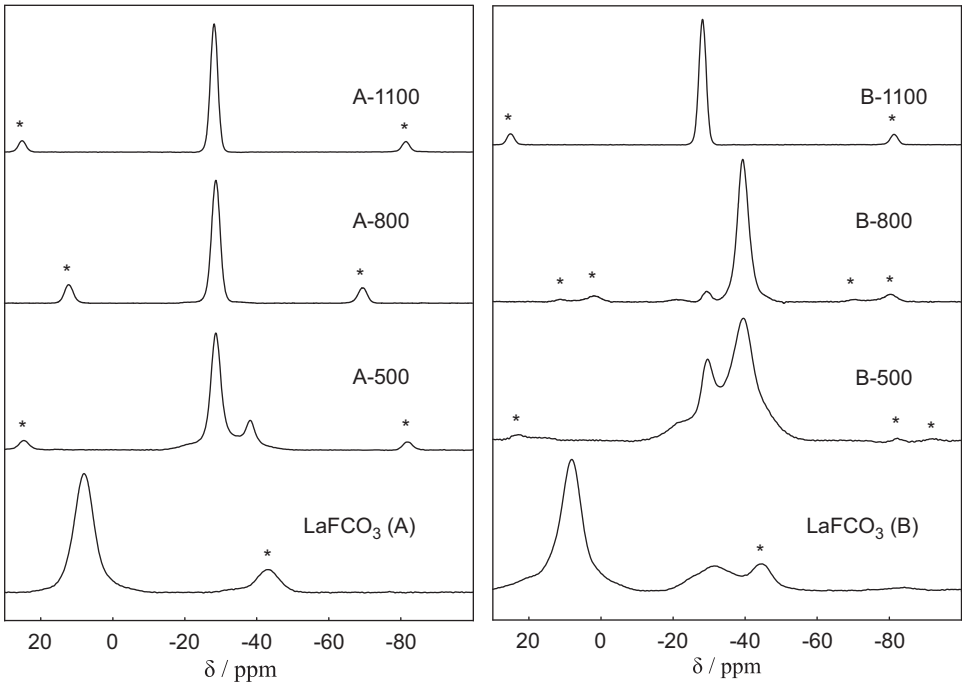

Fig. 3. ^{19}F MAS NMR spectra of samples obtained by thermal decomposition of $LaFCO_3$ (A) and (B) powders for 5 h in air at various temperatures. The asterisks denote spinning side bands.

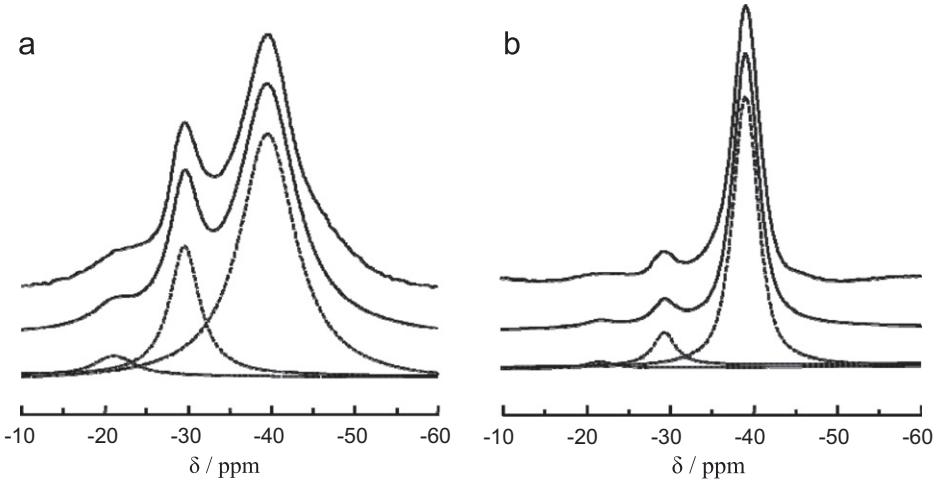

Fig. 4. Experimental (upper) and simulated (lower) ^{19}F MAS NMR spectra of (a) B-500 and (b) B-800. Each spectrum was deconvoluted into three components (dotted lines).

their average particle size of *ca.* 70 nm, while the particles of B-800 were larger than those of A-800.

3.2. Luminescence properties of $LaFCO_3$:Eu^{3+} and LaOF:Eu^{3+} powders

There was no difference between the luminescence spectra of $LaFCO_3$ (A) and (B):Eu^{3+} powders. The spectrum (Fig. 6(a)) of $LaFCO_3$:Eu^{3+} exhibited two distinct peaks at 592 and 616 nm, attributable to $^5D_0 \rightarrow {}^7F_1$ and $^5D_0 \rightarrow {}^7F_2$ transitions, respectively. The former peak was more intense than the latter peak as for YF_3:Eu^{3+} [23] and LaF_3:Eu^{3+} [24], indicating the inversion symmetry of the Eu^{3+} site. The peak corresponding to the $^5D_0 \rightarrow {}^7F_0$ transition was negligibly weak because the transition is allowed only for C_s, C_n, and C_{nv} symmetries [8]. Fig. 6 (b) and (c) show the luminescence spectra of rhombohedral- and tetragonal-LaOF:Eu^{3+}, respectively. The spectra were in accord with those [3,6,8] reported earlier, indicating that the Eu^{3+} ions occupied sites with the symmetries C_{3v} and C_{4v} in rhombohedral- and tetragonal-LaOF:Eu^{3+}, respectively. The low intensity of the $^5D_0 \rightarrow {}^7F_0$ transition peak for rhombohedral-LaOF:Eu^{3+} can be explained by the effect of the T_d pseudosymmetry for the Eu^{3+} site [8].

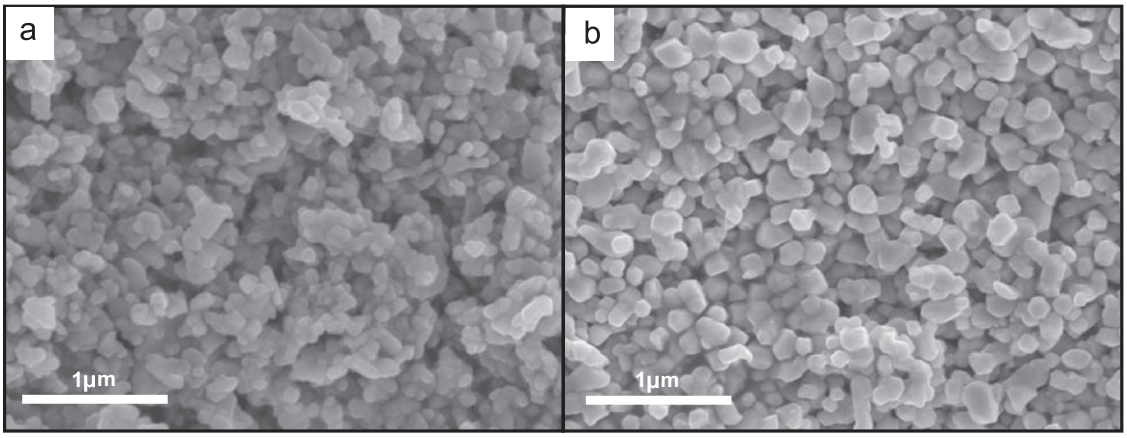

Fig. 5. SEM images of (a) rhombohedral- and (b) tetragonal-LaOF powders obtained at 800 °C.

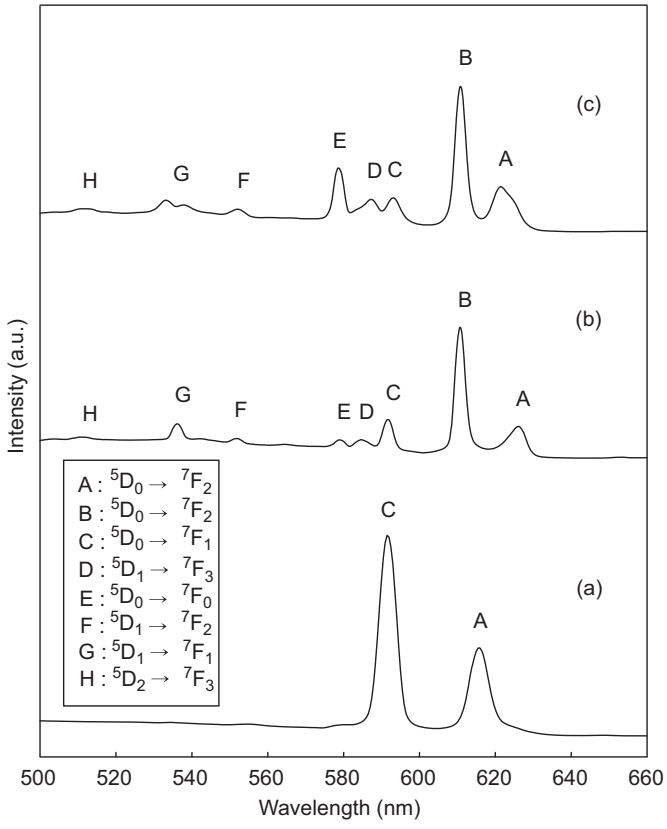

Fig. 6. Luminescence spectra of (a) $LaFCO_3:Eu^{3+}$ ($\lambda_{ex}=396$ nm), and (b) rhombohedral- and (c) tetragonal-$LaOF:Eu^{3+}$ powders ($\lambda_{ex}=363$ nm).

4. Conclusions

This study results demonstrated that ^{19}F MAS NMR spectroscopy is a powerful tool to identify the crystal structure of LaOF powders. The LaOF powders were prepared by thermal decomposition of $LaFCO_3$ powders which had been obtained from boiling an aqueous solution containing lanthanum(III) salt, F^- ion, and urea. $LaFCO_3$ was thermally decomposed into LaOF around 500 °C and the crystal structure (rhombohedral, tetragonal) of LaOF depended on the mole ratio of F^- to La^{3+} ions in the preparation of $LaFCO_3$. The tetragonal-LaOF was completely transformed into rhombohedral-LaOF at 1000 °C. The difference in crystal structures was reflected in the luminescence spectra of the Eu^{3+}-doped LaOF powders.

Acknowledgments

This work was supported by the Energy Efficiency & Resources Program of the Korea Institute of Energy Technology Evaluation and Planning (KETEP) grant (No. 2011T100100081) funded by the Korean Ministry of Knowledge Economy. The ^{19}F MAS NMR spectra were recorded at the Analysis Research Division, Daegu Center, Korea Basic Science Institute.

References

[1] D. Gao, H. Zheng, X. Zhang, Z. Fu, Z. Zhang, Y. Tian, M. Cui, Efficient fluorescence emission and photon conversion of LaOF: Eu^{3+} nanocrystals, Applied Physics Letters 98 (2011) 011907.

[2] X. Zhang, D. Gao, L. Li, Down- and up-conversion luminescence of Tm^{3+}/Ho^{3+} codoped LaOF nanoparticles, Journal of Applied Physics 107 (2010) 123528.

[3] T. Grzyb, S. Lis, Structural and spectroscopic properties of $LaOF:Eu^{3+}$ nanocrystals prepared by the sol–gel Pechini method, Inorganic Chemistry 50 (2011) 8112–8120.

[4] L. Armelao, G. Bottaro, L. Bovo, C. Maccato, M. Pascolini, C. Sada, E. Soini, E. Tondella, Luminescent properties of Eu-doped lanthanum oxyfluoride sol–gel thin films, Journal of Physical Chemistry C 113 (2009) 14429–14434.

[5] Y.-P. Du, Y.-W. Zhang, L.-D. Sun, C.-H. Yan, Luminescent monodisperse nanocrystals of lanthanide oxyfluorides synthesized from trifluoroacetate precursors in high-boiling solvents, Journal of Physical Chemistry C 112 (2008) 405–415.

[6] E. He, H. Zheng, Z. Zhang, X. Zhang, L. Xu, Z. Fu, Y. Lei, Influence of crystal structure on the fluorescence emission of Eu^{3+}:LaOF nanocrystals, Journal of Nanoscience and Nanotechnology 10 (2010) 1908–1912.

[7] O. Janka, T. Schleid, Facile synthesis of bastnaesite-type $LaF[CO_3]$ and its thermal decomposition to LaOF for bulk and Eu^{3+}-doped sample, European Journal of Inorganic Chemistry 2009 (2009) 357–362.

[8] J. Hölsä, Effect of non-stoichiometry on the luminescence properties of lanthanum oxyfluoride, Acta Chemica Scandinavica 45 (1991) 583–587.
[9] S. Fujihara, T. Kato, T. Kimura, Sol–gel synthesis and luminescence properties of oxyfluoride LaOF:Eu^{3+} thin films, Journal of Materials Science Letters 20 (2001) 687–689.
[10] C.T. Au, Y.Q. Zhang, H. He, S.Y. Lai, C.F. Ng, The characterization of $BaCO_3$-modified LaOF catalysts for the OCM reaction, Journal of Catalysis 167 (1997) 354–363.
[11] K.T. Jacob, V.S. Saji, Y. Waseda, Lanthanum oxyfluorides: structure, stability, and ionic conductivity, International Journal of Applied Ceramic Technology 3 (2006) 312–321.
[12] J.W. Fergus, H.P. Chen, Structure and conductivity of tetragonal and rhombohedral lanthanum oxyfluoride compounds, Journal of Electrochemical Society 147 (2000) 4696–4704.
[13] J. Lee, Q. Zhang, F. Saito, Mechanochemical synthesis of lanthanum oxyfluoride from lanthanum oxide and lanthanum fluoride, Journal of the American Chemical Society 84 (2001) 863–865.
[14] T. Petzel, V. Marx, B. Horman, Thermodynamics of the rhombohedral–cubic phase transition of ROF with R≡Y, La, Pr, Nd, Sm–Er, Journal of Alloys and Compounds 200 (1993) 27–31.
[15] S.N. Achary, B.R. Ambekar, M.D. Mathews, A.K. Tyagi, P.N. Moorthy, Study of phase transition and volume thermal expansion in a rare-earth (RE) oxyfluoride system by high-temperature XRD (RE=La, Nd, Sm, Eu and Gd), Thermochimica Acta 320 (1998) 239–243.
[16] J. Hölsä, E. Silynoja, H. Rahiala, J. Valkonen, Characterization of the non-stoichiometry in lanthanum oxyfluoride by FT-IR absorption, Raman scattering, X-ray powder diffraction and thermal analysis, Polyhedron 16 (1997) 3421–3427.
[17] J. Lee, Q. Zhang, F. Saito, Synthesis of nano-sized lanthanum oxyfluoride powders by mechanochemical processing, Journal of Alloys and Compounds 348 (2003) 214–219.
[18] S.E. Dutton, D. Hirai, R.J. Cava, Low temperature synthesis of LnOF rare-earth oxyfluoride through reaction of oxides with PTFE, Materials Research Bulletin 47 (2012) 714–718.
[19] W.H. Zachariasen, Crystal chemical studies of the 5f-series of elements. XIV. Oxyfluorides, XOF, Acta Crystallographica 4 (1951) 231.
[20] F. Wang, C.P. Grey, Probing the mechanism of fluoride-ion conduction in LaF_3 and strontium-doped LaF_3 with high-resolution ^{19}F MAS NMR, Chemistry of Materials 9 (1997) 1068–1070.
[21] F. Wang, C.P. Grey, Probing the defect structure of anion-excess $Ca_{1-x}Y_xF_{2+x}$ (x=0.03–0.32) with high-resolution ^{19}F magic-angle spinning nuclear magnetic resonance spectroscopy, Chemistry of Materials 10 (1998) 3081–3091.
[22] J.W. Fergus, Crystal structure of lanthanum oxyfluoride, Journal of Materials Science Letters 16 (1997) 267–269.
[23] R. Yan, Y. Li, Down/up conversion in Ln^{3+}-doped YF_3 nanocrystals, Advanced Functional Materials 15 (2005) 763–770.
[24] P. Li, Q. Peng, Y. Li, Dual-mode luminescent colloidal spheres from monodispersive rare-earth fluoride nanocrystals, Advanced Materials 21 (2009) 1945–1948.